Hospital population density and risk of respiratory infection : Is close contact density dependent ?

George Shirreff, Anne C.M. Thiébaut, Bich-Tram Huynh, Guillaume Chelius, Antoine Fraboulet, Didier Guillemot, Lulla Opatowski, Laura Temime

Epidemics 49 (2024) 100807

Contents lists available at ScienceDirect

Epidemics

journal homepage: www.elsevier.com/locate/epidemics

Hospital population density and risk of respiratory infection: Is close contact density dependent?

George Shirreff [a,b,c,*], Anne C.M. Thiébaut [b], Bich-Tram Huynh [a,b], NODS-Cov2 Investigation Group [1], Guillaume Chelius [d], Antoine Fraboulet [d], Didier Guillemot [a,b,e], Lulla Opatowski [a,b,2], Laura Temime [c,f,2]

[a] Institut Pasteur, Université Paris Cité, Epidemiology and Modelling of Antibiotic Evasion, Paris, France
[b] Université Paris-Saclay, UVSQ, Inserm, CESP, France
[c] Modélisation, épidémiologie et surveillance des risques sanitaires (MESuRS), Conservatoire National des Arts et Métiers, Paris, France
[d] INRIA, Lyon, France
[e] Department of Public Health, Medical Information, Clinical Research, AP-HP, Paris Saclay, Paris, France
[f] PACRI Unit, Institut Pasteur, Conservatoire national des Arts et Métiers, Paris, France

ARTICLE INFO

Keywords:
Nosocomial infection
Respiratory infection
Close proximity contact
Frequence dependence
Density dependence
Force of infection

ABSTRACT

Respiratory infections acquired in hospital depend on close contact, which may be affected by hospital population density. Models of infectious disease transmission typically assume that contact rates are independent of density (frequency dependence) or proportional to it (linear density dependence), without justification. We evaluate these assumptions by measuring contact rates in hospitals under different population densities. We analysed data from a study in 15 wards in which staff, patients and visitors carried wearable sensors which detected close contacts. We proposed a general model, non-linear density dependence, and fit this to data on several types of interactions. Finally, we projected the fitted models to predict the effect of increasing population density on epidemic risk. We identified considerable heterogeneity in density dependence between wards, even those with the same medical specialty. Interactions between all persons present usually depended little on the population density. However, increasing patient density was associated with higher rates of patient contact for staff and for other patients. Simulations suggested that a 10 % increase in patient population density would carry a markedly increased risk in many wards. This study highlights the variance in density dependent dynamics and the complexity of predicting contact rates.

1. Introduction

The transmission of airborne pathogens such as SARS-CoV-2, Influenza, RSV or resistant bacteria continues to present a risk to patients in healthcare settings (Almasaudi, 2018; Ng et al., 2022; Özen et al., 2023), in spite of the introduction of effective hygiene methods such as masks (Chu et al., 2020) and hydroalcoholic gel (Kratzel et al., 2020). Droplet transmission requires close proximity contacts between infectious and susceptible individuals (Jayaweera et al., 2020), while aerosol transmission is more likely within close proximity (Tang et al., 2021). Knowing the factors that influence the occurrence of those contacts is important in understanding the risk of nosocomial outbreaks. Such contact may occur between two individuals for a specific medical function, during casual contact e.g. socialising, or unintentionally e.g. waiting on adjacent chairs, and this may influence how often and for how long it occurs.

Mathematical models of infectious disease transmission generally rely on the assumption of homogeneous mixing among all individuals in the population. A fundamental question in developing such homogeneous mixing models is the dependency between the density of the population and the force of infection (de Jong et al., 1995; McCallum et al., 2001). We assume that such a dependency occurs through the contact rate (Box 1a).

The most common assumption is frequency dependence (FD) in

* Correspondence to: Institut Pasteur, 25-28 rue du Dr Roux, Paris 75015, France.
E-mail address: george.shirreff@pasteur.fr (G. Shirreff).
[1] See Acknowledgements for a list of members.
[2] Contributed equally.

https://doi.org/10.1016/j.epidem.2024.100807
Received 24 July 2024; Received in revised form 15 November 2024; Accepted 25 November 2024
Available online 29 November 2024

which the number of potentially infectious contacts is independent of the population density, which is typically considered appropriate for sexually transmitted infections (Lloyd-Smith et al., 2004), among many other types of infections. The other common assumption is linear density dependence (LDD), usually referred to simply as "density dependence", although we reserve that term here for any non-zero dependence on density. This is more appropriate for pathogens which spread during unconstrained contacts between individuals. While these can be considered assumptions on a spectrum of density dependence, very few studies have considered an in-between case (Box 1b). However, this has implications for modelling a population with changing population size: if the number of individuals increases while the prevalence of infectiousness stays the same, this would increase the risk under LDD, but not under FD (Box 1c).

Over the last 20 years, most infectious disease modelling studies have assumed either FD or LDD, without verifying the realism or exploring the effect of this assumption (Hopkins et al., 2020). Only 2 studies have explored these assumptions on data involving directly transmitted human pathogens (Bjørnstad et al., 2002; Hu et al., 2013). Bjørnstad et al. found that pre-vaccination measles dynamics in British cities most closely resembled FD transmission (Bjørnstad et al., 2002), while Hu et al. found that a non-linear density dependence (NDD) best explained the transmission of the 1918 influenza across US states (Hu et al., 2013).

A review of 100 papers modelling SARS-CoV-2 transmission in the general population up to June 2020 found that 70 % assumed FD, and 30 % LDD, with none allowing for NDD or flexible density dependence (Nightingale et al., 2021). The authors followed this review by fitting transmission models to the COVID-19 mortality rate in UK local authority areas under different assumptions of population density dependence, when this density was perturbed by social distancing guidelines. In addition to FD and LDD, the authors fitted a third model, that of saturating density dependence in which the transmission rate increased non-linearly with increasing population density, up to an asymptotic maximum transmission rate. They found that this saturating model provided the best fit to the data, while acknowledging that mortality rates may have many different contributing factors beyond changes in contact rate. Crucially, their paper demonstrates that the use of FD models overestimated, and LDD models underestimated, the effect on mortality rates of increasing population density.

In healthcare settings, to our knowledge, this question has never been explored, despite a high frequency and intensity of contacts between individuals (patients and health care workers) and high epidemic risk (Temime et al., 2020). Studies have been conducted to identify the rate at which patients and types of hospital staff come into close contact (Duval et al., 2018; Najafi et al., 2017), and more recently in a context of COVID-19 pandemic (Shirreff et al., 2024). Here, after a systematic review of modelling studies of SARS-CoV-2 transmission in healthcare

A Force of infection in a Susceptible-Infectious-Recovered transmission model

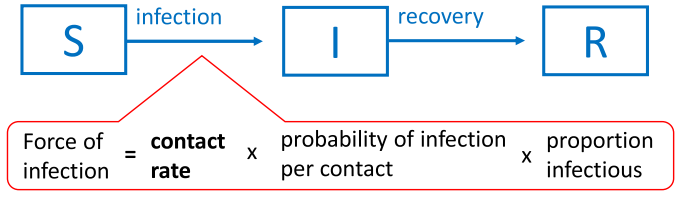

In a homogeneous mixing transmission model, the force of infection is proportional to the contact rate, as well as to the proportion of the population who are infectious (I/N, where $N = S + I + R$).

We assume that population density may directly affect the contact rate, but not the probability of infection per contact or the proportion infectious.

B Spectrum of density dependence of contact rate

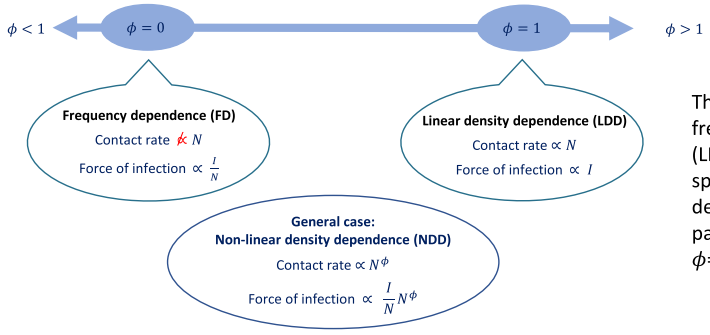

The two most common assumptions for such models are frequency dependence (FD) and linear density dependence (LDD). Both assumptions can be considered points on a spectrum of density dependence. A general case, non-linear density dependence (NDD) can be written, in which the index parameter ϕ governs the position on the spectrum, such that ϕ=0 representing FD, and ϕ=1 LDD.

C Implications of different density dependence assumptions for decreasing or increasing populations

$$R_0 \propto \text{Force of infection} \propto \frac{I}{N}N^{\phi}$$

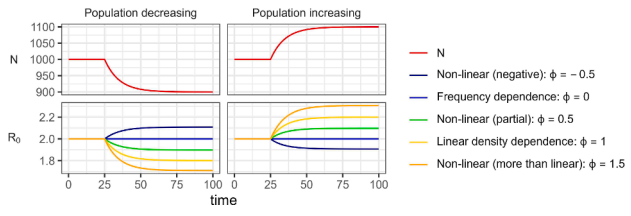

We show here how these assumptions affect the basic reproduction number R_0 (which is also proportional to the force of infection), in a population which decreases to 90% (left) or increases to 110% (right). We assume that the prevalence of infection in those arriving or leaving is the same as the rest of the population. Complete details of the SIR model are given in Supplementary Methods.

When the index parameter ϕ is 0, the population change has no effect on R_0. However, if ϕ is positive, then an increasing population will increase the R_0 while a decreasing population will decrease it. Conversely, under a negative value of ϕ, an increasing population will decrease R_0 and *vice versa*.

Box 1. Explanation of common assumptions around density dependence, with an illustration of the general case.

with regards to their assumptions about FD or LDD dynamics, we interrogate this question through the analysis of data providing detailed information on close proximity interactions over a 36 h period between hospital users, collected in 15 French hospital wards. We conducted the analysis at the level of the ward, and across all wards in aggregate.

2. Materials and methods

2.1. Literature review

We categorised the density dependence assumptions papers modelling the spread of SARS-CoV-2 in healthcare, using the list analysed in a review article (Smith et al., 2023). Based on our examination of the methods section in each paper, their transmission dynamics were categorised as FD, LDD, non-linear, or based on empirical estimates of contact rate.

2.2. Dataset

Data on close proximity contact patterns were collected during April-June 2020 across 15 hospital wards with a range of specialties in eight university hospitals across Paris (including one paediatric hospital), Lyon and Bordeaux (Shirreff et al., 2024). These wards included three in infectious diseases, two in geriatrics, two in adult emergency, two in medical intensive care units (ICUs), one in surgical ICU, one in internal medicine, one in pneumology, and three wards in a dedicated pediatric hospital: general pediatrics, emergency and neonatal ICU.In order to minimise the potential effect of weekend days on staffing and admissions, studies in all wards began on days from Monday to Friday, with only two beginning on Friday and therefore overlapping with the weekend.

Wearable sensors were offered to all individuals on entering or leaving the ward, including patients, visitors and healthcare workers (HCW). The times at which sensors were given to and recovered from participants were recorded. The sensors detected the presence of other sensors every 10 s within approximately 1.5 m, and recorded the identity of the other sensor and the duration of the contact. Further details on the study population have been published previously (Shirreff et al., 2024).

2.3. Population density

The study period was divided up into time windows between instances of arrival or departure of any participant, during which the population size was constant. The recorded times at which sensors were given and recovered was used to identify the number of persons present, N_w, during each time window w. It was assumed that the functional area of the ward did not change during the study period, meaning that the number of persons present could be assumed to represent the population density.

In order to prevent possible artefacts introduced into the data during the short period during which the sensors were being distributed or recuperated, in which the apparent density was low but the true density (including those who did not have active sensors) may have been higher, we excluded time windows at the start and end of the study when the numbers of active sensors were low. For the main analysis, all data collected at the beginning of the study period before the first 10 sensors were active on the ward, or at the end of the study period after the final 10 sensors were active, were discarded.

2.4. Contact rates

As one person can have multiple simultaneous contacts, we define the contact rate as the total number of cumulative minutes in contact for a person, per minute that they spend on the ward.

Within each time window w, the observed contact rate c_w^{obs} is calculated from the total contact time across all participants, where m_{iw} is the total cumulative number of minutes in contact for individual i in time window w, divided this by the total person minutes in which these events can occur, being the product of the number of persons present and the duration of the time window d_w.

$$c_w^{\text{obs}} = \frac{\sum_{i}^{N_w} m_{iw}}{N_w d_w}$$

2.5. Model for NDD contact rates

We propose a model which captures FD, LDD and NDD dynamics with a single non-linearity index parameter ϕ. This determines how the contact rate during a time window w would be affected by the population density during that time window.

The contact rate during time window w, c_w, is modelled as follows:

$$c_w = a(\phi) {N_w}^{\phi}$$

where $a(\phi)$ is a scaling parameter specific to that dataset and that value of ϕ. Under this model, a value of $\phi = 0$ is equivalent to FD, $\phi = 1$ is equivalent to LDD, and other values represent NDD, being partially density dependent for $0 < \phi < 1$, but with values of both $\phi < 0$ (negative density dependence) or $\phi > 1$ (more than linear density dependence) also being possible (Box 1b).

The contact rate model is calibrated for a given dataset and given value of ϕ using the scaling parameter $a(\phi)$ such that the total contact time T over all time windows and individuals present is the same for the observed and modelled contacts:

$$T = \sum_w c_w^{\text{obs}} N_w d_w = \sum_w c_w N_w d_w$$

The value of T can be calculated from observed data simply as the total cumulative contact time across all individuals and time windows:

$$T = \sum_{iw} m_{iw}$$

The contact rate model is substituted into this equation to give;

$$T = \sum_{iw} m_{iw} = \sum_w a(\phi) {N_w}^{\phi} N_w d_w$$

This can be rearranged to calculate the scaling parameter $a(\phi)$ as follows:

$$a(\phi) = \frac{\sum_{iw} m_{iw}}{\sum_w {N_w}^{\phi} N_w d_w}$$

2.6. Statistical inference

The likelihood $\mathscr{L}(w, \phi)$ of observing a given contact rate c_w^{obs} in time window w is calculated according to an exponential distribution with mean c_w (equivalent to rate $\frac{1}{c_w}$). This likelihood function was chosen because the distribution of c_w^{obs} in each ward takes the form of an exponential distribution.

The total log likelihood for this value of ϕ is calculated by summing the log likelihood over all time windows.

$$L(\phi) = \sum_w \log(\mathscr{L}(w, \phi))$$

Non-linear index parameters and their 95 % credibility intervals were estimated using a Markov Chain Monte Carlo algorithm from the *FME* package in *R* (R Core Team, 2022; Soetaert and Petzoldt, 2010). A normal prior with standard deviation 1 was used to favour the most plausible values in situations with few datapoints, and with mean 0.5 in order to be agnostic between the FD and LDD models. No statistical

inference was required for fitting of the FD and LDD models, as the value of ϕ was fixed at 0 and 1, respectively.

2.7. Diurnal models

Under the assumption that night and day time behaviours may be different, we conducted analyses in which we separated the time windows which began during the day time (08:00–19:59) from those that began in the night time (20:00–07:59). For each time period p, a separate value of the index, ϕ_p and the scaling parameter $a\left(\phi_p\right)$, were estimated.

The total likelihood for an index ϕ_p was calculated by summing the log likelihood over all time windows falling within time period p, and this value was used for inference of ϕ_p. The overall likelihood of a diurnal model for model comparison was calculated by summing the log likelihood over all day and night time windows, using the best ϕ_p value in each period p.

2.8. Subsetting contact rates

Some analyses targeted specific populations. For those, we considered only the contacts that individuals of type x formed with individuals of type y (e.g. HCW forming contacts with patients), and during a specific time period p such as day or night time.

The observed contact rate is subset, where the relevant population size in window w, N_{wx}, is that of the type forming contacts, x, and m_{iyw} is the total minutes of contact formed by individual i (of type x) with all individuals of type y in time window w.

$$c_{wxy}^{\text{obs}} = \frac{\sum_{i \in x}^{N_w} m_{iyw}}{N_{wx} d_w}$$

The rate at which type x contacts type y during time window w, c_{wxy}, is then modelled as follows, where the relevant population size N_{wy} is of that type with whom contacts are being formed, y, and where time window w falls within period p.

$$c_{wxy} = a_{xyp}(\phi_{xyp}) N_{wy}{}^{\phi_{xyp}} \text{ for any } w \in p$$

The contact formation model is calibrated using the scaling parameter $a_{xyp}(\phi_{xyp})$ for that value of ϕ_{xyp} such that the total contact time between x and y in time period p, T_{xyp}, is the same for modelled observed contacts.

$$T_{xyp} = \sum\nolimits_{w \in p} c_{wxy}^{\text{obs}} N_{wx} d_w = \sum\nolimits_{w \in p} c_{wxy} N_{wx} d_w$$

This can be rearranged to calculate the scaling parameter for that subset of contacter, contactee and time period, and for the specific value of ϕ_{xyp}.

$$a_{xyp}(\phi_{xyp}) = \frac{\sum_{i \in x}^{N_w} m_{iyw}}{\sum_w N_{wy}{}^{\phi_{xyp}} N_{wx} d_w}$$

The likelihood $\mathscr{L}(w, \phi_{xyp})$ of observing the contact rate c_{wxy}^{obs}, is calculated according to an exponential distribution with mean c_{wxy} (equivalent to rate $\frac{1}{c_{wxy}}$).

The total log likelihood for this value of ϕ_{xyp} is then calculated by summing the log likelihood over all time windows in period p.

$$L(\phi_{xyp}) = \sum_{w \in p} \log\left(\mathscr{L}_{(w, \phi_{xyp})}\right)$$

2.9. Aggregating all wards

The analysis was primarily conducted on each ward separately. We additionally conducted an analysis with data from all wards aggregated, and estimated a single value of ϕ and the scaling parameter $a(\phi)$ for the non-diurnal models, or values ϕ_p and the scaling parameters $a\left(\phi_p\right)$ for the diurnal models.

2.10. Models for comparison

Details of all models to be tested against the data are given in Table 1.

The model likelihood for all types of contacter and contactee and non-diurnal models was calculated according to the likelihood across all time windows with $\widehat{\phi}$, the most likely value of ϕ.

Model likelihood $= L(\widehat{\phi})$

In models with only contacter type x and contactee type y, the overall likelihood for non-diurnal models was calculated according to the likelihood across all time windows with $\widehat{\phi_{xy}}$, the most likely value of ϕ_{xy}.

Model likelihood$_{xy}$ $= L\left(\widehat{\phi_{xy}}\right)$

In diurnal models including all types of contacter and contactee, the overall model likelihood was calculated by summing the likelihoods for both time periods, each with the best value index parameter

Model likelihood$_{\text{diurnal}}$ $= \sum_{p=day,night} L\left(\widehat{\phi_p}\right)$

or with specific contacter and contactee combinations

Model likelihood$_{\text{diurnal}x,y}$ $= \sum_{p=day,night} L\left(\widehat{\phi_{xyp}}\right)$

Model comparison was conducted using AIC:

$AIC = 2k - 2 *$ Model likelihood$_{\blacksquare}$

and for each ward the $dAIC$ was calculated as the difference in AIC relative to the best model.

2.11. Sensitivity analysis

We conducted a sensitivity analysis in which the threshold of sensors required at the beginning or end of the study was modified: this was by default 10, but we repeated the analysis with a threshold of 0 (no exclusion) or 20 sensors. We also repeated analysis of diurnal models in which the start of the day period was 04:00, 06:00 and 10:00, in addition to the principle analysis in which the day started at 08:00.

Table 1
Models of density dependence in contact rate.

Model	Non-linearity index parameter (s), $\phi_{\blacksquare}$	Scaling parameter (s), $a(\phi_{\blacksquare})$	Diurnality	Number of estimated parameters (k)
Frequency dependence	Set at 0	One calibrated	Non-diurnal: same dynamic across day and night time	1
Linear density dependence	Set at 1	One calibrated		1
Non-linear density dependence	One estimated	One calibrated		2
Frequency dependent - diurnal	Set at 0	Two calibrated	Diurnal: index and scaling parameters estimated separately for day (08:00–19:59) and night time.	2
Linear density dependence - diurnal	Set at 1	Two calibrated		2
Non-linear density dependence - diurnal	Two estimated	Two calibrated		4

2.12. Overcrowding scenario

In order to examine the effect a change in population density would have on the epidemic risk, we proposed a hypothetical scenario in which the population density increased by 10 %, and evaluated the change in expected contact rate under the best-fit model.

This was calculated for a population of type x making contact with type y during time period p as follows:

$$(\text{Contact rate increase under 10\% population increase})_{xyp} = 1.1^{\phi_{xyp}} - 1$$

3. Results

3.1. Literature review

We conducted a review to examine how nosocomial SARS-CoV-2 transmission is modelled in the literature. Of 40 papers which describe dynamic models of nosocomial transmission published up to February 2022, 25 assumed FD (Baek et al., 2020; Booton et al., 2021; Bosbach et al., 2021; Ding et al., 2021; Evans et al., 2021a; Gómez Vázquez et al., 2022; Gudina et al., 2021; Hall et al., 2021; Holmdahl et al., 2022, 2021; Huang et al., 2021; Kahn et al., 2022; Litwin et al., 2022; Love et al., 2021a, 2021b; Lucia-Sanz et al., 2023; Martos et al., 2020; Nguyen et al., 2021a, 2021b; Obama et al., 2021; Pham et al., 2021; Rosello et al., 2022; Runge et al., 2022; Schmidt et al., 2022; Wilmink et al., 2020) and 11 assumed LDD (Dy and Rabajante, 2020; Evans et al., 2021b; Fosdick et al., 2022; Hollinghurst et al., 2022; Kluger et al., 2020; Lasser et al., 2021; Qiu et al., 2021; Sanchez-Taltavull et al., 2021; Sánchez-Taltavull et al., 2021; See et al., 2021; Zhang and Cheng, 2020). No papers assumed partial density dependence or NDD. The remaining 4 papers used empirically measured contact networks, so no additional assumption was necessary (Hüttel et al., 2021; Smith et al., 2020; Tofighi et al., 2021; Vilches et al., 2021).

3.2. Size of dataset

Across the 15 wards, 2114 individuals (1320 HCW, 573 patients and 221 visitors) participated in the study for a total of 1,374,902 min spent on the wards with active sensors. These recorded a total of 33,946 unique contacts, lasting a total of 333,542 min. Average contact rate was 0.15 contact minutes per person minute spent on the ward, with ward-level averages ranging from 0.08 to 0.26. The distribution of contact rates among all time windows appeared broadly exponential across all wards (Supplementary Fig. S 1).

3.3. Model comparison

When the analysis was conducted by ward on all individuals present in the hospital, the most frequently selected model was the diurnal non-linear density-dependent model, favoured in 7/15 wards (Table 2). The remaining 8 wards favoured a non-diurnal model, of which 5 favoured a frequency-dependent model, 2 favoured a linear density-dependent model, and 1 a non-linear model.

When we focused on contacts with patients only, the non-linear diurnal model was favoured in the majority of wards, both when considering contacts formed by HCW with patients (Table 3, 9 wards out of 15) or by patients with other patients (Table 4, 6 wards out of 11).

Overall, the emergency wards (adult and paediatric) favoured a non-linear diurnal model, whereas within other ward specialties (ICUs, Geriatry, Infectious Diseases) the best model was not consistent between different wards with the same specialty.

When all wards were analysed in aggregate, the best model was the non-diurnal frequency-dependent model.

3.4. Estimated density dependence

When we estimated the parameters of the contact rate model for each ward and across all types of interactions, we found that, even in cases where the best-fit model was non-linear, the estimated index parameter was close to or its 95 % credibility interval included zero (Fig. 1), implying close to frequency-dependent interactions overall. Night time interactions tended to exhibit somewhat more density dependence, as did HCW contacts with patient, but remained overall much closer to frequency than to density dependence. However, interactions between patients tended to display much more density dependence, even when the interactions were aggregated across all wards (Fig. 1). In many wards the contact rates had a greater than linear relationship with the population size of patients. In some wards there were no interactions between patients and therefore this could not be estimated.

There were also many instances of apparent negative relationships between population density and contact rate. These can be seen in comparison to the data (Fig. 2), for example in Medical ICU #2, the Adult emergency wards during the day, and Paediatric emergency during the night. Many instances where the frequency dependent model was the best may have favoured this model because a model with monotonic change in relation to population density did not capture the changing contact rate (Fig. 2, Supplementary Fig. S 1 and Supplementary Fig. S 2). The range of possible slopes estimated for non-linear models is shown in Supplementary Fig. S 3.

When we considered contacts formed with patients by specific types

Table 2
Comparison of models of contact rate between all persons on each ward. Each row represents a ward, and each column a model. For a given model the dAIC value is given relative to the best model for each ward (indicated by dAIC = **0**).

Diurnal or non-diurnal	Non-diurnal			Diurnal		
Ward	Frequency dependent	Linear density dependence	Non-linear	Frequency dependent	Linear density dependence	Non-linear
Adult emergency #1	19.5	342.2	16.4	7.6	337.6	**0**
Adult emergency #2	14.7	349.8	14.8	9.4	347.7	**0**
General paediatrics	26.1	38.3	23.0	28.0	26.5	**0**
Geriatry #1	**0**	200.5	2.0	3.2	158.4	5.7
Geriatry #2	5.0	507.9	5.9	68.3	715.0	**0**
Infectious diseases #1	65.7	52.2	49.8	65.9	46.2	**0**
Infectious diseases #2	**0**	122.5	1.3	15.7	126.6	8.1
Infectious diseases #3	**0**	407.8	1.5	1.7	333.7	2.6
Internal medicine	16.7	**0**	1.3	12.8	0.8	3.9
Medical ICU #1	5.4	417.7	**0**	9.6	267.6	0.2
Medical ICU #2	25.5	492.5	13.8	14.1	486.6	**0**
Neonatal ICU	**0**	411.2	0.6	14.6	428.4	4.4
Paediatric emergency	6.7	253.0	8.4	7.4	152.7	**0**
Pneumology	**0**	162.8	1.7	0.8	71.7	4.5
Surgical ICU	34.9	**0**	1.7	43.8	9.3	13.3
All wards	**0**	3696.3	1.0	47.7	3107.8	34.0

Table 3
Comparison of models of contact rate when HCW form contacts with patients, on each ward. Each row represents a ward, and each column a model. For a given model (columns) the dAIC value is given relative to the best model for each ward (indicated by dAIC = **0**).

Diurnal or non-diurnal	Non-diurnal			Diurnal		
Ward	Frequency dependent	Linear density dependence	Non-linear	Frequency dependent	Linear density dependence	Non-linear
Adult emergency #1	183.8	859.2	151.8	173.3	900.9	**0**
Adult emergency #2	47.1	651.8	48.5	52.3	735.4	**0**
General paediatrics	53.7	47.5	47.5	44.8	38.9	**0**
Geriatry #1	**0**	49.9	1.6	2.0	34.9	3.4
Geriatry #2	**0**	134.9	0.9	11.6	97.5	9.6
Infectious diseases #1	10.0	2.0	0.5	12.8	**0**	3.2
Infectious diseases #2	74.4	189.7	76.4	62.7	168.4	**0**
Infectious diseases #3	**0**	208.8	1.7	5.6	185.1	8.8
Internal medicine	8.5	79.9	**0**	4.2	36.5	3.3
Medical ICU #1	18.5	23.9	3.5	17.1	26.9	**0**
Medical ICU #2	3.3	91.3	5.3	**0**	95.1	0.1
Neonatal ICU	45.3	970.2	24.2	17.2	778.6	**0**
Paediatric emergency	52.9	29.5	11.0	48.6	13.9	**0**
Pneumology	155.1	1531.1	98.5	156.8	1562.3	**0**
Surgical ICU	80.9	24.9	7.1	81.0	27.1	**0**
All wards	9.0	4194.0	**0**	14.0	3904.2	6.0

Table 4
Comparison of models of contact rate when patients form contacts with other patients, on each ward. Each row represents a ward, and each column a model. For a given model (columns) the dAIC value is given relative to the best model for each ward (indicated by dAIC = 0). Results are missing for four wards as there were no contacts between patients.

Diurnal or non-diurnal	Non-diurnal			Diurnal		
Ward	Frequency dependent	Linear density dependence	Non-linear	Frequency dependent	Linear density dependence	Non-linear
Adult emergency #1	165.9	472.6	61.9	159.9	448.4	**0**
Adult emergency #2	391.8	333.2	277.1	322.5	224.5	**0**
General paediatrics	45.1	28.9	27.4	50.9	28.6	**0**
Geriatry #1	12.2	74.4	10.1	13.8	75.2	**0**
Geriatry #2	272.6	1221.3	82.0	7.9	**0**	2.6
Infectious diseases #1	-	-	-	-	-	-
Infectious diseases #2	-	-	-	-	-	-
Infectious diseases #3	19.3	138.0	19.3	24.8	145.7	**0**
Internal medicine	74.1	40.7	**0**	71.5	40.5	6.0
Medical ICU #1	143.4	94.7	**0**	149.7	101.5	13.2
Medical ICU #2	-	-	-	-	-	-
Neonatal ICU	-	-	-	-	-	-
Paediatric emergency	108.5	164.7	110.4	68.7	119.3	**0**
Pneumology	18.0	**0**	2.0	7.9	1.9	2.7
Surgical ICU	137.0	90.4	**0**	146.1	97.1	7.4
All wards	591.8	53.0	**0**	620.9	57.4	1.3

of staff, we observed that although there was much variation between wards, nurses and auxiliary nurses generally experienced more density dependent contacts with patients, with many instances of more than linear density dependence (Fig. 3). Physicians experienced more highly density-dependent contacts, as did administration staff, although there were many wards in which these specific models were not estimable due to lack of contact with patients.

3.5. Sensitivity analysis

Varying the threshold number of activated sensors (Supplementary Table S 1) or the period considered to be daytime (Supplementary Table S 2) did not have systematic effects on the best-fit model for each ward, which remained quite consistent.

3.6. Overcrowding scenario

In order to illustrate the implications for nosocomial risk, we calculated the expected increase in contact rate for day and night time in each ward, based on its best fit model, under a scenario of 10 % increase in population density (Fig. 4). While the majority of wards would experience only small changes in contact rates between all persons present, there were exceptions such as the General paediatrics and Infectious diseases #1 wards where the model predicted a more than 10 % increase. When considering how a change in the patient density would impact contact with patients, many more wards would exhibit a greater than 30 % increase in contact rate. For those wards with a negative non-linear fit however, the increase in population density would correspond to a reduction in contact rate.

4. Discussion

We explored here the patterns of density dependence in hospital contacts based on unique real-world data on interactions between individuals in hospitals. We exploited data collected from proximity sensors in several types of hospitals over day and night shifts and between types of hospital users, we examined the contact rates and how these evolved under changing population density.

The dependency of contact rates on population density was highly heterogeneous between wards, without evident associations with the types of wards, the hospital housing the ward or the city. We identified many wards and scenarios in which contact rates appeared to depend little on the density, suggesting frequency-dependent dynamics. However, night time contacts were generally more density dependent than daytime ones.

Interactions that HCW form with patients, and patients with other

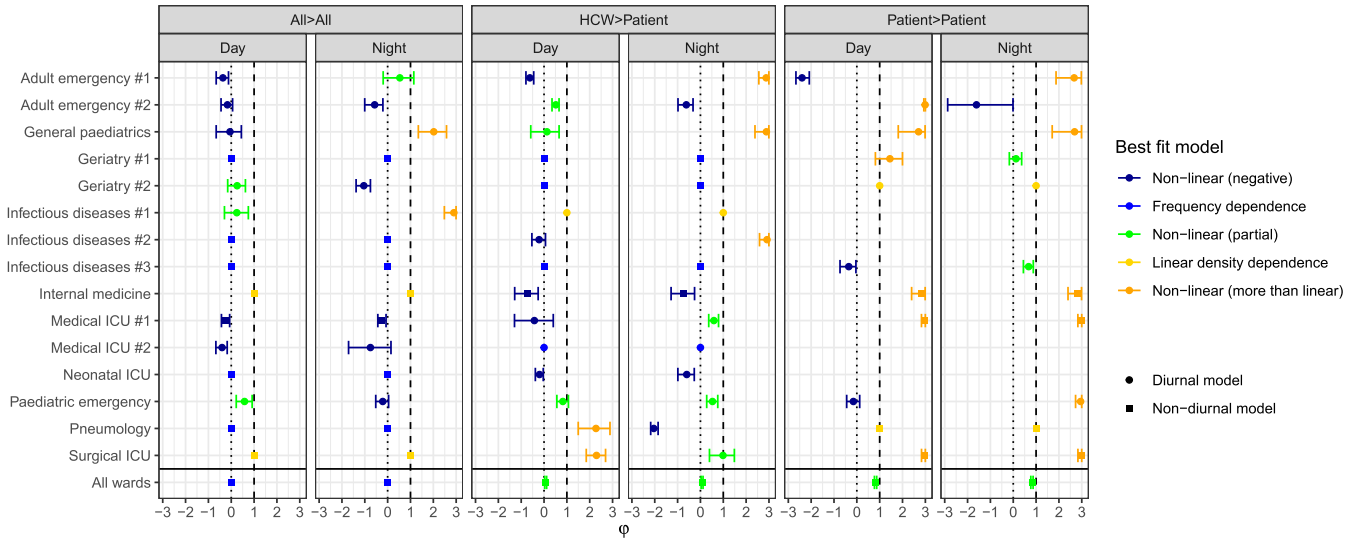

Fig. 1. Estimated values of ϕ for each ward under different types of contact or time period. Each row represents a ward, and each column represents either the day or night time, with each pair of columns representing a type of contact (between all person present; when HCW form contacts with patients; or patients with other patients). The colours represent the best fit model, and the points represent the median estimate of ϕ under each scenario. If the best fit model is non-linear, the value of ϕ is estimated, and therefore the 95 % credibility interval is shown by the error bars. If the best fit model is frequency dependence and linear density dependence, the value of ϕ is fixed and only the point is shown. Circular points indicate that the best fit model is diurnal, while square points indicate non-diurnal. The vertical dotted and dashed lines respectively indicate the values for $\phi = 0$ for frequency dependence and $\phi = 1$ for linear density dependence.

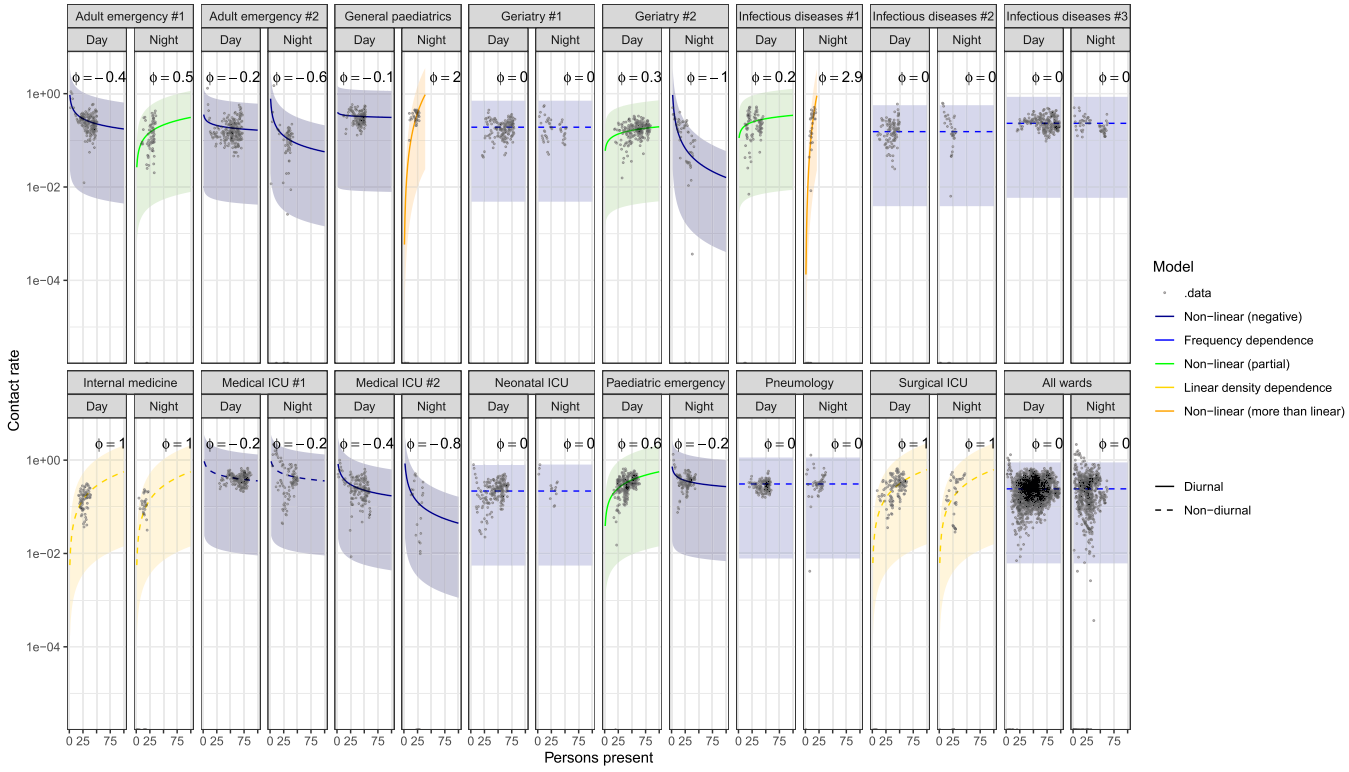

Fig. 2. Correlation between contact rates and number of persons present on the ward. Each pair of panels represents the day and night time on each ward. The black points indicate the data, being contact rates (cumulative contact minutes per person minute spent on the ward) against number of persons present on the ward, for each time window. The coloured lines indicate the best fit model, with solid and dashed lines indicating diurnal and non-diurnal models, respectively. The shaded band represents the 95 % confidence interval of the exponential distribution around the best-fit rate.

patients, exhibited higher density dependence, implying that contact rates were sensitive to increasing numbers of patients. This effect was particularly strong for interactions that nurses and auxiliary nurses formed with patients. Interestingly, another study using wearable sensors in an emergency department identified higher numbers of contacts during periods of high population density in patient-patient and HCW-patient interactions (Hertzberg et al., 2017), although in our study the results varied between the emergency wards.

Frequency dependence predominated when the wards were analysed in aggregate, which is consistent with previous work identifying

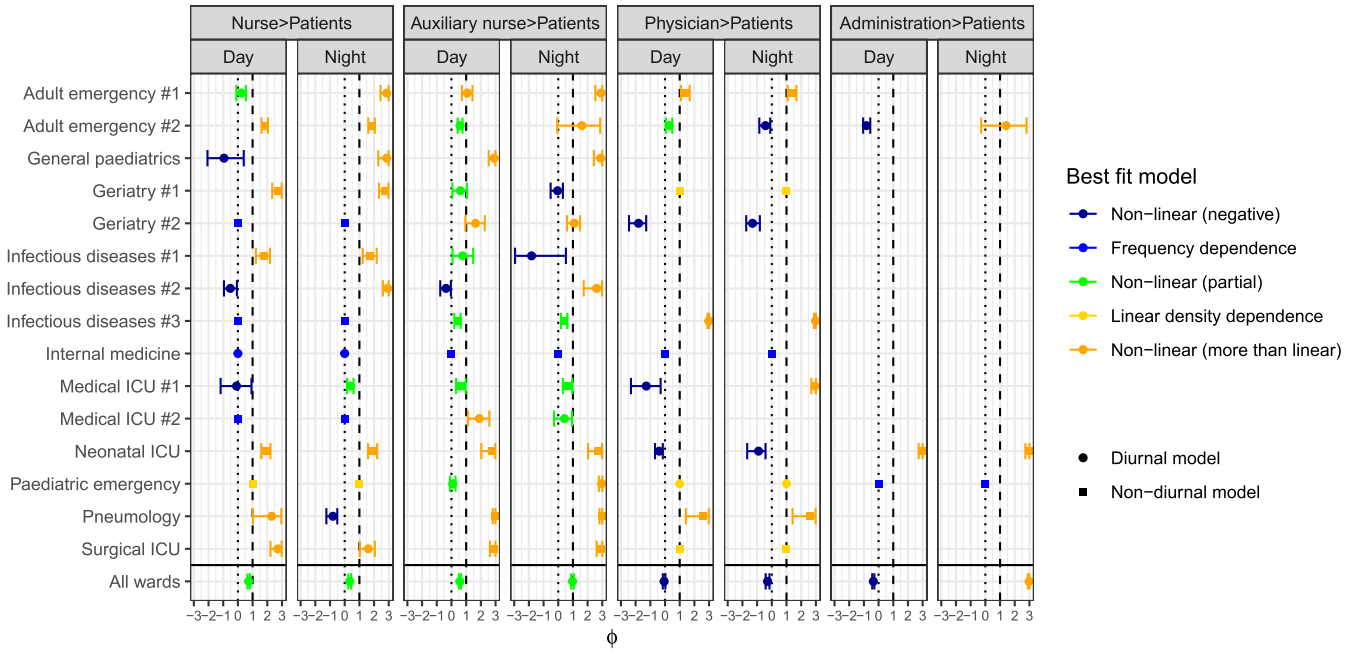

Fig. 3. Estimated values of ϕ for each ward by time period and type of HCW forming contacts with patients. Each row represents a ward, and each column represents either the day or night time, with each pair of columns representing a type of contact with patients (by nurses; auxiliary nurses; physicians; and administration staff). The colours represent the best fit model, and the points represent the median estimate of ϕ under each scenario. If the best fit model is non-linear, the value of ϕ is estimated, and therefore the 95 % credibility interval is shown by the error bars. If the best fit model is frequency dependence and linear density dependence, the value of ϕ is fixed and only the point is shown. Circular points indicate that the best fit model is diurnal, while square points indicate non-diurnal. The vertical dotted and dashed lines respectively indicate the values for $\phi = 0$ for frequency dependence and $\phi = 1$ for linear density dependence.

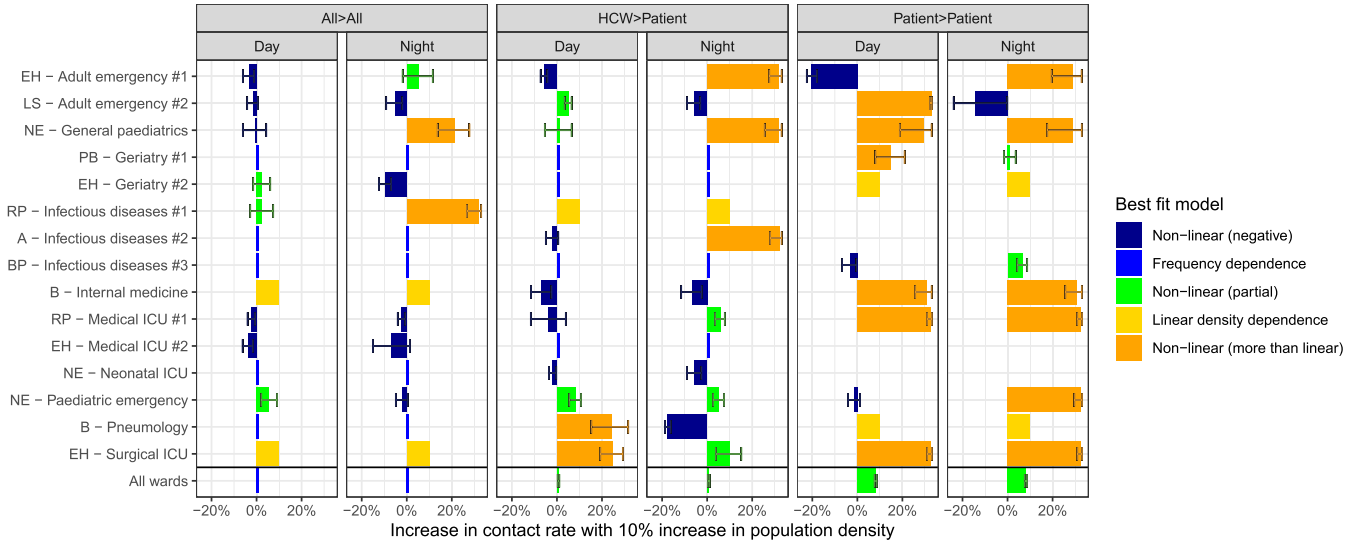

Fig. 4. Simulated effect on contact rate of an increase in population density. Each row represents a ward, and each column represents either the day or night time, with each pair of columns representing a type of contact (between all person present; when HCW form contacts with patients; or patients with other patients). The colours represent the best fit model, and the bars represent the increase in contact rate expected if the population density were to increase by 10 %. Where a non-linear model was the best fit, we have included error bars to demonstrate the limits of the increase in contact rate corresponding to the 95 % credibility limits of the estimate of ϕ.

frequency dependence at large spatial scales despite local density dependence (Ferrari et al., 2011). Intuitively it is perhaps unsurprising that the analysis across wards did not reveal a strong relationship with population density, given the heterogeneity of results between wards.

Under these best fit models, we simulated a scenario in which population density increased by 10 %, reflecting hospital overcrowding. While many wards would exhibit little change in contact rate, some others could demonstrate an increase in contact rate much greater than the population density increase, potentially leading to markedly increased epidemic risk.

Our review of healthcare transmission models in the literature revealed a predominance in the assumption of FD over LDD, which is consistent with our results if the choice between these two models is binary. This predominance was also reflected in an earlier review of SARS-CoV-2 transmission models in the community (Nightingale et al., 2021). However, our results suggest that empirically there is great

variation in the best model across the spectrum of density dependence, and while some studies used empirically estimated contact rates, these were in the minority, and none used a partially density dependent scenario.

We acknowledge that, if studies do not model a changing population density, then the choice of density dependence model is moot. However, hospital populations do fluctuate, particularly due to seasonal patterns of admission (Achebak et al., 2023; Upshur et al., 2005), suggesting that modelling such changes is important. This dynamic was particularly the case under a pandemic scenario in which COVID-19 drove people into hospitals, while cancellation of unrelated medical interventions drove people out.

This study provides a unique insight into these questions, by combining a rich dataset on contact patterns with a flexible formulation for translating this into changes in epidemiological risk. The data were collected across all types of persons present within several hospital wards, over more than a day, and achieved very high coverage. We were even able to examine density dependence among specific staff roles in each ward. The formulation allowed us to estimate whether these contact scenarios correspond to frequency dependence, linear density dependence, or some other relationship on this spectrum, which can be directly linked to models of epidemiological transmission. We acknowledge that other functional forms may govern the dependency between population density and contact rate, such as a saturating relationship, where the change of contact rate with increasing population density decelerates as it approaches an asymptotic value, or a sigmoidal relationship in which the increase of contact rate with population density is highest at intermediate population densities. However, we have chosen to use a simpler single model framework, NDD, which maps to the main assumptions present in the literature (FD and LDD) in order to best assess their appropriateness.

The results must be interpreted in the light of certain assumptions and limitations. We assumed that all contacts are equal in terms of epidemiology, whereas in reality some may be much riskier than others. We do not have information on whether participants were wearing masks or subject to other barrier methods, even though this is likely to be relevant for epidemic risk (Shirreff et al., 2022). We also discount the possibility that infection status influences contact behaviour, such as by isolation of patients with COVID-19. Intriguingly, mask use may also respond to population density, which would be a fruitful area for further research.

We also do not consider the social fluidity i.e. whether a person's cumulative contact is with a few or with many people, which would often be relevant for the risk of spread, since many short contacts increases the risk that one of these contacts is infected (Colman et al., 2021). However, estimates of social fluidity do not take into account the duration of these contacts, and without knowing the prevalence of infectious index cases, or the saturation of risk during long contact with the same person, our approach provides a better link to overall risky contact time. Contact data such as we analyse here can be used to produce contact networks, which can be extended by simulation (Duval et al., 2024), allowing models of disease transmission which take into account both contact rates and repeat contacts. Importantly, the data collection was conducted during the end of the first COVID-19 wave (April–June 2020), which may imply that it doesn't represent "normal" contact behaviour, but instead a scenario in which individuals may be particularly avoidant due to fear of infection. However, given the pressures put on to healthcare institutions during the COVID-19 pandemic, understanding the contact and density dynamics at such times is relevant for future disruptive events.

The models that we fit to data were not always able to capture the complexity of the changing contact rate. This may depend on other things than just population density, such as shift patterns and scheduled activities. Relatedly, we have assumed an equal duration of day time and night time periods for our diurnal models. However, we provide a general framework which produces a simple, easy to understand analysis which can be applied to other scenarios such as changes in hospital organisation which may affect population density.

Finally, we leveraged the daily change in population density to extrapolate about the effect of longer-term changes in population density. Extension of this analysis to studies which have collected longer term data (Duval et al., 2018) would be relevant to generalising these results, including longer-term fluctuations in population density, and beyond those affected by the COVID-19 pandemic. Collection of more details on patients and ward activities would allow a more detailed analysis of the correlates of high and low contact rates, in addition to the population density. The inclusion in future work of the surface area of the wards, which was unavailable for the current study, would allow the extension of relative measures of population density to absolute measures, enabling better comparisons between wards.

5. Conclusions

Changing population density has a substantial effect on contact rates in many scenarios. However, the effect varies between wards and according to the types of actors involved, and is in many cases non-linear. Overall contact rates often had low or no dependency on density, suggesting that FD models are appropriate for modelling generalised hospital transmission. However, contacts with patients, and contacts at night time, were more density dependent. Understanding this is key to anticipating hospital crowding as a risk factor for nosocomial outbreaks, as well as informing our assumptions in epidemic models. We propose further work to reveal how longer term changes in population density affect contact rate, and how they affect relevant contact behaviours such as mask use.

CRediT authorship contribution statement

Bich-Tram Huynh: Supervision, Investigation, Data curation. **Anne C.M. Thiébaut:** Writing – review & editing, Methodology. **George Shirreff:** Writing – review & editing, Writing – original draft, Visualization, Validation, Software, Methodology, Formal analysis, Data curation, Conceptualization. **Laura Temime:** Writing – review & editing, Methodology, Formal analysis, Conceptualization. **Antoine Fraboulet:** Methodology, Investigation. **Guillaume Chelius:** Methodology, Investigation. **Lulla Opatowski:** Writing – review & editing, Supervision, Methodology, Formal analysis, Conceptualization. **Didier Guillemot:** Writing – review & editing, Supervision, Project administration, Methodology, Investigation, Funding acquisition, Formal analysis, Conceptualization.

Funding

Funding was provided by

- Fondation de France (MODCOV project grant 106059) as part of the alliance framework "Tous unis contre le virus" (LO).
- Université Paris-Saclay (AAP Covid-19 2020) (LO).
- The French government through its National Research Agency project Nods-Cov-2 ANR-20-COVI-0026-01 (DG) and SPHINX ANR-17-CE36-0008-01 (LT).

Declaration of Competing Interest

The authors declare the following financial interests/personal relationships which may be considered as potential competing interests: George Shirreff reports a relationship with Sanofi that includes: funding grants. If there are other authors, they declare that they have no known competing financial interests or personal relationships that could have appeared to influence the work reported in this paper.

Acknowledgements

The NODS-Cov2 Investigation Group includes the following members:

Assistance Publique – Hôpitaux de Paris: Djillali Annane, Aurélien Dinh, Olivier Lambotte, Sophie Bulifon, Magali Guichardon, Sebastien Beaune, Julie Toubiana, Elsa Kermorvant-Duchemin, Gerard Chéron, Hugues Cordel; **Hospices Civils de Lyon**: Laurent Argaud, Marion Douplat, Paul Abraham, Karim Tazarourte, Géraldine Martin-Gaujard, Philippe Vanhems, Delphine Hilliquin; **Centre Hospitalier Universitaire de Bordeaux**: Duc Nguyen.

We would like to thank: Nawal Derridj-Ait Younes, Naima Sghiouar, Tanga Vanessa Ntouba Christianne, Sylvie Azerad and Théo Debert from the clinical research unit of the Paris-Saclay university hospital; Gaetane Niel, Ga Han Park, Audrey Vallerix, Cypriane Tazi, Loueli Ouballa, Valentine Le Cardonnel, Lou Davaine, Madeleine Dutheil de la Rochère, Adeline Alleau, Tiphaine Biaggi, Manuela Carrico, Antoine Goudour, Pauline Jaubert, Marion Galliou, Mathilde de Menthon, Noémie Chanson for their participation in the field investigation.

Appendix A. Supporting information

Supplementary data associated with this article can be found in the online version at doi:10.1016/j.epidem.2024.100807.

Data availability

The data and codes used for this analysis (as specified in the manuscript) can be found at github.com/georgeshirreff/FreqDensDep.

References

Achebak, H., Garcia-Aymerich, J., Rey, G., Chen, Z., Méndez-Turrubiates, R.F., Ballester, J., 2023. Ambient temperature and seasonal variation in inpatient mortality from respiratory diseases: a retrospective observational study. Lancet Reg. Health - Eur. 35, 100757.

Almasaudi, S.B., 2018. Acinetobacter spp. as nosocomial pathogens: epidemiology and resistance features. Saudi J. Biol. Sci. 25 (3), 586–596.

Baek, Y.J., Lee, T., Cho, Y., Hyun, J.H., Kim, M.H., Sohn, Y., et al., 2020. A mathematical model of COVID-19 transmission in a tertiary hospital and assessment of the effects of different intervention strategies. PLoS One 15 (10), e0241169.

Bjørnstad, O.N., Finkenstädt, B.F., Grenfell, B.T., 2002. Dynamics of measles epidemics: estimating scaling of transmission rates using a time series sir model. Ecol. Monogr. 72 (2), 169–184.

Booton, R.D., MacGregor, L., Vass, L., Looker, K.J., Hyams, C., Bright, P.D., et al., 2021. Estimating the COVID-19 epidemic trajectory and hospital capacity requirements in South West England: a mathematical modelling framework. BMJ Open 11 (1), e041536.

Bosbach, W.A., Heinrich, M., Kolisch, R., Heiss, C., 2021. Maximization of open hospital capacity under shortage of SARS-CoV-2 vaccines—an open access, stochastic simulation tool. Vaccines 9 (6), 546.

Chu, D.K., Akl, E.A., Duda, S., Solo, K., Yaacoub, S., Schünemann, H.J., et al., 2020. Physical distancing, face masks, and eye protection to prevent person-to-person transmission of SARS-CoV-2 and COVID-19: a systematic review and meta-analysis. Lancet 395 (10242), 1973–1987.

Colman, E., Colizza, V., Hanks, E.M., Hughes, D.P., Bansal, S., 2021. Social fluidity mobilizes contagion in human and animal populations. In: Hens, N., Davenport, M. P., Saramaki, J., Hens, N. (Eds.), eLife, e62177.

Ding, Y., Agrawal, S.K., Cao, J., Meyers, L., Hasenbein, J.J., 2021. Surveillance testing for rapid detection of outbreaks in facilities. arXiv:211000170 [q-bio, stat] [Internet]. [cited 2022 Jan 7]; Available from: ⟨http://arxiv.org/abs/2110.00170⟩.

Duval, A., Leclerc, Q.J., Guillemot, D., Temime, L., Opatowski, L., 2024. An algorithm to build synthetic temporal contact networks based on close-proximity interactions data. PLoS Comput. Biol. 20 (6), e1012227.

Duval, A., Obadia, T., Martinet, L., Boëlle, P.Y., Fleury, E., Guillemot, D., et al., 2018. Measuring dynamic social contacts in a rehabilitation hospital: effect of wards, patient and staff characteristics. Sci. Rep. 8 (1), 1686.

Dy, L.F., Rabajante, J.F., 2020. A COVID-19 infection risk model for frontline health care workers. Netw. Model. Anal. Health Inf. Bioinform. 9 (1), 57.

Evans, S., Agnew, E., Vynnycky, E., Stimson, J., Bhattacharya, A., Rooney, C., et al., 2021a. The impact of testing and infection prevention and control strategies on within-hospital transmission dynamics of COVID-19 in English hospitals. Philos. Trans. R. Soc. B: Biol. Sci. 376 (1829), 20200268.

Evans, S., Stimson, J., Pople, D., Bhattacharya, A., Hope, R., White, P.J., et al., 2021b. Quantifying the contribution of pathways of nosocomial acquisition of COVID-19 in English hospitals. Int. J. Epidemiol. Dec 4;dyab241.

Ferrari, M.J., Perkins, S.E., Pomeroy, L.W., Bjørnstad, O.N., 2011. Pathogens, social networks, and the paradox of transmission scaling. Interdiscip. Perspect. Infect. Dis. 2011, e267049.

Fosdick, B.K., Bayham, J., Dilliott, J., Ebel, G.D., Ehrhart, N., 2022. Model-based evaluation of policy impacts and the continued COVID-19 risk at long term care facilities. Infect. Dis. Model. 7 (3), 463–472.

Gómez Vázquez, J.P., García, Y.E., Schmidt, A.J., Martínez-López, B., Nuño, M., 2022. Testing and vaccination to reduce the impact of COVID-19 in nursing homes: an agent-based approach. BMC Infect. Dis. 22 (1), 477.

Gudina, E.K., Ali, S., Girma, E., Gize, A., Tegene, B., Hundie, G.B., et al., 2021. Seroepidemiology and model-based prediction of SARS-CoV-2 in Ethiopia: longitudinal cohort study among front-line hospital workers and communities. Lancet Glob. Health 9 (11), e1517–e1527.

Hall, I., Lewkowicz, H., Webb, L., House, T., Pellis, L., Sedgwick, J., et al., 2021. Outbreaks in care homes may lead to substantial disease burden if not mitigated. Philos. Trans. R. Soc. B: Biol. Sci. 376 (1829), 20200269.

Hertzberg, V.S., Baumgardner, J., Mehta, C.C., Elon, L.K., Cotsonis, G., Lowery-North, D. W., 2017. Contact networks in the emergency department: effects of time, environment, patient characteristics, and staff role. Soc. Netw. 48, 181–191.

Hollinghurst, J., North, L., Emmerson, C., Akbari, A., Torabi, F., Williams, C., et al., 2022. Intensity of COVID-19 in care homes following hospital discharge in the early stages of the UK epidemic. Age Ageing 51 (5), afac072.

Holmdahl, I., Kahn, R., Hay, J.A., Buckee, C.O., Mina, M.J., 2021. Estimation of transmission of COVID-19 in simulated nursing homes with frequent testing and immunity-based staffing. JAMA Netw. Open 4 (5), e2110071.

Holmdahl, I., Kahn, R., Slifka, K.J., Dooling, K., Slayton, R.B., 2022. Modeling the impact of vaccination strategies for nursing homes in the context of increased severe acute respiratory syndrome coronavirus 2 community transmission and variants. Clin. Infect. Dis. 75 (1), e880–e883.

Hopkins, S.R., Fleming-Davies, A.E., Belden, L.K., Wojdak, J.M., 2020. Systematic review of modelling assumptions and empirical evidence: does parasite transmission increase nonlinearly with host density? Methods Ecol. Evol. 11 (4), 476–486.

Hu, H., Nigmatulina, K., Eckhoff, P., 2013. The scaling of contact rates with population density for the infectious disease models. Math. Biosci. 244 (2), 125–134.

Huang, Q., Mondal, A., Jiang, X., Horn, M.A., Fan, F., Fu, P., et al., 2021. SARS-CoV-2 transmission and control in a hospital setting: an individual-based modelling study. R. Soc. Open Sci. 8 (3), 201895.

Hüttel, F.B., Iversen, A.M., Hansen, M.B., Ersbøll, B.K., Ellermann-Eriksen, S., Olsen, N. L., 2021. Analysis of social interactions and risk factors relevant to the spread of infectious diseases at hospitals and nursing homes. PLoS One 16 (9), e0257684.

Jayaweera, M., Perera, H., Gunawardana, B., Manatunge, J., 2020. Transmission of COVID-19 virus by droplets and aerosols: a critical review on the unresolved dichotomy. Environ. Res, 188, 109819.

de Jong, M.C.M., de Diekmann, O., Heesterbeek, J.A.P., 1995. How does transmission of infection depend on population size. Publ. Newton Inst. 5, 84–94.

Kahn, R., Holmdahl, I., Reddy, S., Jernigan, J., Mina, M.J., Slayton, R.B., 2022. Mathematical modeling to inform vaccination strategies and testing approaches for coronavirus disease 2019 (COVID-19) in nursing homes. Clin. Infect. Dis. 74 (4), 597–603.

Kluger, D.M., Aizenbud, Y., Jaffe, A., Parisi, F., Aizenbud, L., Minsky-Fenick, E., et al., 2020. Impact of healthcare worker shift scheduling on workforce preservation during the COVID-19 pandemic. Infect. Control Hosp. Epidemiol. 41 (12), 1443–1445.

Kratzel, A., Todt, D., V'kovski, P., Steiner, S., Gultom, M., Thao, T.T.N., et al., 2020. Inactivation of severe acute respiratory syndrome coronavirus 2 by WHO-recommended hand rub formulations and alcohols. Emerg. Infect. Dis. 26 (7), 1592–1595.

Lasser, J., Zuber, J., Sorger, J., Dervic, E., Ledebur, K., Lindner, S.D., et al., 2021. Agent-based simulations for protecting nursing homes with prevention and vaccination strategies. J. R. Soc. Interface 18 (185), 20210608.

Litwin, T., Timmer, J., Berger, M., Wahl-Kordon, A., Müller, M.J., Kreutz, C., 2022. Preventing COVID-19 outbreaks through surveillance testing in healthcare facilities: a modelling study. BMC Infect. Dis. 22 (1), 105.

Lloyd-Smith, J.O., Getz, W.M., Westerhoff, H.V., 2004. Frequency-dependent incidence in models of sexually transmitted diseases: portrayal of pair-based transmission and effects of illness on contact behaviour. Proc. Biol. Sci. 271 (1539), 625–634.

Love, J., Keegan, L.T., Angulo, F.J., McLaughlin, J.M., Shea, K.M., Swerdlow, D.L., et al., 2021a. Continued need for non-pharmaceutical interventions after COVID-19 vaccination in long-term-care facilities. Sci. Rep. 11 (1), 18093.

Love, J., Wimmer, M.T., Toth, D.J.A., Chandran, A., Makhija, D., Cooper, C.K., et al., 2021b. Comparison of antigen- and RT-PCR-based testing strategies for detection of SARS-CoV-2 in two high-exposure settings. PLoS One 16 (9), e0253407.

Lucia-Sanz, A., Magalie, A., Rodriguez-Gonzalez, R., Leung, C.Y., Weitz, J.S., 2023. Modeling shield immunity to reduce COVID-19 transmission in long-term care facilities. Ann. Epidemiol. 77, 44–52.

Martos, D.M., Parcell, B.J., Eftimie, R., Martos, D.M., Parcell, B.J., Eftimie, R., 2020. Modelling the transmission of infectious diseases inside hospital bays: implications for COVID-19. MBE 17 (6), 8084–8104.

McCallum, H., Barlow, N., Hone, J., 2001. How should pathogen transmission be modelled? Trends Ecol. Evol. 16 (6), 295–300.

Najafi, M., Laskowski, M., de Boer, P.T., Williams, E., Chit, A., Moghadas, S.M., 2017. The effect of individual movements and interventions on the spread of influenza in long-term care facilities. Med. Decis. Mak. 37 (8), 871–881.

Ng, C.Y.H., Lim, N.A., Bao, L.X.Y., Quek, A.M.L., Seet, R.C.S., 2022. Mitigating SARS-CoV-2 transmission in hospitals: a systematic literature review. Public Health Rev. 43, 1604572.

Nguyen, L.K.N., Howick, S., McLafferty, D., Anderson, G.H., Pravinkumar, S.J., Meer, R. V.D., et al., 2021b. Impact of visitation and cohorting policies to shield residents from covid-19 spread in care homes: an agent-based model. Am. J. Infect. Control 49 (9), 1105–1112.
Nguyen, L.K.N., Howick, S., McLafferty, D., Anderson, G.H., Pravinkumar, S.J., Meer, R. V.D., et al., 2021a. Evaluating intervention strategies in controlling coronavirus disease 2019 (COVID-19) spread in care homes: an agent-based model. Infect. Control Hosp. Epidemiol. 42 (9), 1060–1070.
Nightingale, E.S., Brady, O.J., Group, C.C. 19 working, Yakob, L., 2021. The importance of saturating density dependence for population-level predictions of SARS-CoV-2 resurgence compared with density-independent or linearly density-dependent models, England, 23 March–31 July 2020. Eurosurveillance 26 (49), 2001809.
Obama, H.C.J.T., Yousif, N.A.M., Nemer, L.A., Ngougoue, P.M.N., Ngwa, G.A., Teboh-Ewungkem, M., et al., 2021. Preventing COVID-19 spread in closed facilities by regular testing of employees—an efficient intervention in long-term care facilities and prisons? PLoS One 16 (4), e0249588.
Özen, S., Özgür Horoz Ö, Öztürk, G., Sökmen, H., Kandemir, T., Yarkin, F., 2023. The investigation of community-acquired and nosocomial respiratory syncytial virus and other viral respiratory tract infections in children. New. Microbiol. 46 (3), 271–277.
Pham, T.M., Tahir, H., van de Wijgert, J.H.H.M., Van der Roest, B.R., Ellerbroek, P., Bonten, M.J.M., et al., 2021. Interventions to control nosocomial transmission of SARS-CoV-2: a modelling study. BMC Med. 19 (1), 211.
Qiu, X., Miller, J.C., MacFadden, D.R., Hanage, W.P., 2021. Evaluating the contributions of strategies to prevent SARS-CoV-2 transmission in the healthcare setting: a modelling study. BMJ Open 11 (3), e044644.
R Core Team, 2022. R: A Language and Environment for Statistical Computing [Internet]. R Foundation for Statistical Computing, Vienna, Austria. Available from: ⟨https://www.R-project.org/⟩.
Rosello, A., Barnard, R.C., Smith, D.R.M., Evans, S., Grimm, F., Davies, N.G., et al., 2022. Impact of non-pharmaceutical interventions on SARS-CoV-2 outbreaks in English care homes: a modelling study. BMC Infect. Dis. 22 (1), 324.
Runge, M., Richardson, R.A.K., Clay, P.A., Bell, A., Holden, T.M., Singam, M., et al., 2022. Modeling robust COVID-19 intensive care unit occupancy thresholds for imposing mitigation to prevent exceeding capacities. PLoS Glob. Public Health 2 (5), e0000308.
Sanchez-Taltavull, D., Castelo-Szekely, V., Murugan, S., Hamley, J.I.D., Rollenske, T., Ganal-Vonarburg, S.C., et al., 2021. Regular testing of asymptomatic healthcare workers identifies cost-efficient SARS-CoV-2 preventive measures. PLoS One 16 (11), e0258700.
Sánchez-Taltavull, D., Castelo-Szekely, V., Candinas, D., Roldán, E., Beldi, G., 2021. Modelling strategies to organize healthcare workforce during pandemics: application to COVID-19. J. Theor. Biol. 523, 110718.
Schmidt, A.J., García, Y., Pinheiro, D., Reichert, T.A., Nuño, M., 2022. Using non-pharmaceutical interventions and high isolation of asymptomatic carriers to contain the spread of SARS-CoV-2 in nursing homes. Life 12 (2), 180.
See, I., Paul, P., Slayton, R.B., Steele, M.K., Stuckey, M.J., Duca, L., et al., 2021. Modeling effectiveness of testing strategies to prevent coronavirus disease 2019 (COVID-19) in nursing homes—United States, 2020. Clin. Infect. Dis. 73 (3), e792–e798.
Shirreff, G., Huynh, B.T., Duval, A., Pereira, L.C., Annane, D., Dinh, A., et al., 2024. Assessing respiratory epidemic potential in French hospitals through collection of close contact data (April–June 2020). Sci. Rep. 14 (1), 3702.
Shirreff, G., Zahar, J.R., Cauchemez, S., Temime, L., Opatowski, L., 2022. EMEA-MESuRS working group on the nosocomial modelling of SARS-CoV-22. Measuring basic reproduction number to assess effects of nonpharmaceutical interventions on nosocomial SARS-CoV-2 transmission. Emerg. Infect. Dis. 28 (7), 1345–1354.
Smith, D.R.M., Chervet, S., Pinettes, T., Shirreff, G., Jijón, S., Oodally, A., et al., 2023. How have mathematical models contributed to understanding the transmission and control of SARS-CoV-2 in healthcare settings? A systematic search and review. J. Hosp. Infect. S0195-6701(23)00298-0.
Smith, D.R.M., Duval, A., Pouwels, K.B., Guillemot, D., Fernandes, J., Huynh, B.T., et al., 2020. Optimizing COVID-19 surveillance in long-term care facilities: a modelling study. BMC Med. 18 (1), 386.
Soetaert, K., Petzoldt, T., 2010. Inverse modelling, sensitivity and monte carlo analysis in R using package FME. J. Stat. Softw. 33, 1–28.
Tang, J.W., Marr, L.C., Milton, D.K., 2021. Aerosols should not be defined by distance travelled. J. Hosp. Infect. 115, 131–132.
Temime, L., Gustin, M.P., Duval, A., Buetti, N., Crépey, P., Guillemot, D., et al., 2020. A conceptual discussion about R0 of SARS-COV-2 in healthcare settings. Clin. Infect. Dis.
Tofighi, M., Asgary, A., Merchant, A.A., Shafiee, M.A., Najafabadi, M.M., Nadri, N., et al., 2021. Modelling COVID-19 transmission in a hemodialysis centre using simulation generated contacts matrices. PLoS One 16 (11), e0259970.
Upshur, R.E., Moineddin, R., Crighton, E., Kiefer, L., Mamdani, M., 2005. Simplicity within complexity: Seasonality and predictability of hospital admissions in the province of Ontario 1988–2001, a population-based analysis. BMC Health Serv. Res.
Vilches, T.N., Nourbakhsh, S., Zhang, K., Juden-Kelly, L., Cipriano, L.E., Langley, J.M., et al., 2021. Multifaceted strategies for the control of COVID-19 outbreaks in long-term care facilities in Ontario, Canada. Prev. Med. 148, 106564.
Wilmink, G., Summer, I., Marsyla, D., Sukhu, S., Grote, J., Zobel, G., et al., 2020. Real-time digital contact tracing: development of a system to control COVID-19 outbreaks in nursing homes and long-term care facilities. JMIR Public Health Surveill. 6 (3), e20828.
Zhang, Y., Cheng, S.R., 2020. Evaluating the need for routine COVID-19 testing of emergency department staff: quantitative analysis. JMIR Public Health Surveill. 6 (4), e20260.